Magnetic coupling of Fe-porphyrin molecules adsorbed on clean and $c(2 \times 2)$ oxygen-reconstructed Co(100) investigated by spin-polarized photoemission spectroscopy

A. P. Weber,[1,2] A. N. Caruso,[1,*] E. Vescovo,[2] Md. E. Ali,[3,4] K. Tarafder,[4] S. Z. Janjua,[1] J. T. Sadowski,[5] and P. M. Oppeneer[4]

[1]*Department of Physics, University of Missouri-Kansas City, Kansas City, Missouri 64110, USA*

[2]*National Synchrotron Light Source, Brookhaven National Laboratory, Upton, New York 11973, USA*

[3]*Centre for Theoretical Chemistry, Ruhr-Universität, D-44780 Bochum, Germany*

[4]*Department of Physics and Astronomy, Uppsala University, Box 516, S-751 20 Uppsala, Sweden*

[5]*Center for Functional Nanomaterials, Brookhaven National Laboratory, Upton, New York 11973, USA*

(Received 4 March 2013; published 10 May 2013)

The spin-polarized electronic structure of iron octaethylporphyrin (FeOEP) molecules adsorbed on a pristine and on a $c(2 \times 2)$ oxygen-reconstructed Co(100) surface has been analyzed by means of spin-polarized photoemission spectroscopy (SPPES) and first-principles density functional theory with the on-site Coulomb repulsion U term (DFT + U) calculations with and without Van der Waals corrections. The aim is to examine the magnetic exchange mechanism between the FeOEP molecules and the Co(100) substrate in the presence or absence of the oxygen mediator. The results demonstrate that the magnetic coupling from the ferromagnetic substrate to the adsorbed FeOEP molecules is ferromagnetic, whereas, the coupling is antiferromagnetic for the FeOEP on the $c(2 \times 2)$O/Co(100) system. Spin-resolved partial densities of states extracted from *ab initio* DFT + U modeling are in fairly good comparison with the electronic spectral densities seen in angle-integrated SPPES energy dispersion curves for submonolayer coverages of FeOEP. Through combined analysis of these spectra and theoretical results, we determine that hybridization of $2p$ orbitals of N and O with Co $3d$ orbitals facilitates indirect magnetic exchange interactions between Fe and Co, whereas, a direct Fe-Co interaction involving the Fe d_{z^2} orbital is also found for FeOEP on Co. It is observed through SPPES that the spin polarization of the photoemission-visible molecular overlayers decreases to zero as coverage is increased beyond the submonolayer regime, indicating that only interfacial magnetic coupling is at work. Microspot low-energy electron diffraction and low-energy electron microscopy were performed to characterize the physical order of the molecular coverage, revealing that FeOEP structural domains are orders of magnitude greater in size on $c(2 \times 2)$O/Co(100) than on clean Co(100), which coincides with reduced scattering from the disorder and sharper features seen in SPPES.

DOI: 10.1103/PhysRevB.87.184411 PACS number(s): 75.70.Cn, 75.70.Rf, 73.20.Hb, 79.60.Dp

I. INTRODUCTION

The magnetic exchange properties of transition metal (TM) centers in TM complexes depend directly on the competition between d-d electron correlation in the open d shell and the degree of hybridization between localized d and delocalized non-d orbital states.[1] Recent studies of TM-centered molecules with nonzero magnetic moments on TM substrates[2] have highlighted the role of p-d interfacial hybridization[3,4] through its implications on spin-carrier transport.[5,6] A detailed description of the magnetic and electronic properties and how they carry through an interface is, however, complicated by the fact that hybridization can occur not only between TMs of the molecules through ligand-based states, but also between any of the molecule's TM or ligand-based states and those of the substrate,[7,8] yielding a combination and competition of direct versus indirect magnetic exchange.

A notable case where interfacial hybridization has been predicted to have a dramatic influence on the magnetic exchange of a TM complex is that of a metal porphyrin adsorbed on a ferromagnetic (FM) substrate. Results of recent DFT + U (density functional theory with an additional on-site Coulomb repulsion U term) calculations predicted that Fe porphyrin (FeP) adsorbed on ferromagnetic Co(100) assumes a ferromagnetic $S = 1$ configuration due to indirect hybridization of the substrate Co e_g electrons to unpaired Fe e_g electrons through N p_z orbitals.[8,9] DFT + U results also predict that FeP adsorbed atop a single bridging oxygen to ferromagnetic Co(100) assumes an antiferromagnetic (AFM) $S = 3/2$ configuration due to indirect hybridization of Fe and Co mediated by O p_z orbitals.[10] Experimental evidence supporting this interpretation is based on x-ray magnetic circular dichroism spectroscopy studies[8,10–12] which confirm the element-specific local magnetic moments predicted by DFT + U for Fe and Co. The experimental technique, however, cannot elucidate the exchange mechanism through hybrid states directly. Meanwhile, a similar TM-centered molecule/ferromagnet interface, Co-phthalocyanine (CoPc) adsorbed to a ferromagnetic Fe(110) substrate, was studied *via* spin-polarized scanning tunneling microscopy (STM) and DFT-based calculations.[13] The energy-dependent spin information extracted, thereby, was reported to suggest the existence of a spin-split interfacial hybrid state, even though the total magnetic moment on the molecule calculated by DFT is zero. Notably, a different interpretation of the vanishing of the Co local moment has recently been given in terms of a Kondo screening.[14]

Although it has been anticipated by many that interfacial p-d hybridization dominates the exchange and resultant magnetic properties at the interface of TM-centered molecules with ferromagnets, quantitative evidence for this, resolving the spin- and orbital-dependent electronic interactions which define the exchange mechanism(s) at work, is desired. The opposing interpretations for the CoPc adsorption to Fe(110) exemplify a need to consider inspection of orbital hybridizations at low binding energies as directly as possible for clarification. For

these reasons, we have investigated the spin-resolved occupied electronic structure of FeOEP layers adsorbed on a clean Co(100) and on a $c(2 \times 2)$ oxygen-reconstructed Co(100) surface using spin-polarized photoemission spectroscopy (SPPES) and compared directly with the spin-resolved partial densities of states derived from DFT + U calculations; low-energy electron diffraction (LEED) and low-energy electron microscopy (LEEM) were used to confirm the physical order of the substrates and adsorption layers as congruent with the local physical structures used in the calculations.

SPPES reveals that the induced spin polarization between molecules and substrate is only present in the molecular submonolayer range for both FeOEP adsorptions on the Co(100) and O/Co(100) substrates. We further show that the ground state of the FeOEP molecules on the ferromagnetic Co(100) is affected by hybridization to the substrate with Russell-Saunders coupling determined by electron correlation and ligand field effects. Our results demonstrate that the spin-polarized photoemission spectra are well explained by DFT + U theory and suggest that the hybridization of molecular orbitals with substrate states carrying nonzero magnetization is affected by the presence of an exchange layer, oxygen in this case, which reverses the sign of electron-spin polarization and the resulting magnetic moment. Van der Waals (VdW) correction terms, whose influence we assessed by performing calculations with and without such corrections, are found to give rise to a more complex behavior. We find their influence to be very small for FeP on O/Co(001) but considerable for FeP adsorption on the metallic Co substrate, however, without improving the agreement with measured SPPES spectra.

II. EXPERIMENTAL AND CALCULATION DETAILS

All experiments were carried out in ultrahigh vacuum ($p < 2 \times 10^{-10}$ mbar) at the National Synchrotron Light Source (NSLS) beamline U5UA. Thick epitaxial Co layers [$\sim$10 ML (monolayer)] were grown via electron-beam evaporation on a clean Cu(100) single-crystal surface, prepared by repeated Ar^+ sputtering and annealing cycles. LEEM and microspot (spot size of 2-μm) low-energy electron diffraction (μ-LEED) as well as valence-band photoemission spectroscopy were used to characterize the growth of Co(100) films on Cu(100) and the $c(2 \times 2)$ oxygen reconstruction on the Co(100) surface.[15] After room-temperature deposition, the Co films were annealed at 450 K for 5 min to reduce the surface roughness. Sharp $c(2 \times 2)$ reconstructions were observed after dosing the clean Co(100) surface with approximately 4 langmuir of O_2 at room temperature [1 langmuir $\sim 10^{-6}$ Torr s], followed by annealing at 400 K for 5 min. FeOEP films [$C_{36}H_{44}Fe(II)N_4$] were grown *in situ* at 490 K from Fe^{III}-octaethylporphyrin chloride [$C_{36}H_{44}ClFe(III)N_4$] powder using a Knudsen cell onto a substrate held at room temperature following previously reported procedures.[3,4,8,16] It has previously been predicted by DFT + U convergence studies and has been shown by x-ray absorption spectroscopy that chlorine detaches from the Fe coordination center of Fe^{III}-octaethylporphyrin chloride at some point during the adsorption process, yielding only FeOEP at the surface.[8] Such detaching of the axial ligand has been detected, too, in STM studies.[17] The thickness of the FeOEP molecules was estimated by a combination of LEEM images, work function variations, suppression of the substrate emission in the photoemission spectra, as well as growth time following prior reports *vide supra*. The induced spin polarization of the FeOEP molecules on clean and oxygen-covered Co layers was studied by SPPES.[18,19] The photoelectron spectra were collected with a commercial Omicron electron energy analyzer (EA120) equipped with a 30-keV mini-Mott polarimeter for spin analysis. The electron energy analyzer was set at high magnification with $\pm 8^\circ$ angular acceptance, allowing the incident photon flux to be reduced during the measurement so as to minimize beam damage to the molecules. All spectra shown were measured at room temperature with the photoelectrons collected at surface normal using s-polarized incident photons of energy $h\nu = 29$ eV. After each deposition of a chosen coverage, the sample was magnetized by applying a current pulse (corresponding to $\sim$300 Oe of the magnetic field) through small Helmholtz coils surrounding the sample and oriented along the Co(100) easy axis, *in plane* along the [110] direction.

The spin-polarized electronic structures of the FeOEP/Co(100) and FeOEP/$c(2 \times 2)$O/Co(100) heterostructures were modeled using the first-principles DFT + U approach in which the strong on-site d-d electron correlation on the Fe atom is taken into account by the additional on-site Coulomb repulsion U and exchange J terms; in the present calculations, these were chosen as 4 and 1 eV, respectively. These values were previously shown to provide a good description of equilibrium properties and the spin state of gas-phase-ligated TM porphyrins.[9,20,21] The full-potential plane-wave code VASP (Ref. 22) was used as it has been shown to be particularly suited for studying extended magnetic systems on a metallic substrate.[23] The calculations were carried out both with and without inclusion of VdW correction terms.[24,25] A kinetic-energy cutoff of 400 eV was used for the plane waves in the basis set. We performed full geometric optimizations of the porphyrin molecules, including their distance to and positions on the surface, together with a full relaxation of the top substrate layers. Three atomic layers modeled the metallic substrate, whereas, the oxidized surface was modeled with an additional $c(2 \times 2)$ oxygen layer. To reduce the computational effort, the peripheral ethyl end groups were replaced by hydrogen atoms. Reciprocal space sampling was performed using $2 \times 2 \times 2$ Monkhorst-Pack k points. For the DFT part of the functional, we employed the generalized-gradient approximation within the Perdew-Burke-Ernzerhof parametrization.[26]

III. RESULTS AND DISCUSSION

A. Electronic and atomic structure: PES and μ-LEED results

The evolution of the valence-band spectra with increasing coverage of the FeOEP molecules is shown in Fig. 1. The electron dispersion curves in the top panel refer to adsorption of FeOEP on the clean Co metal substrate, whereas, those in the bottom show the result of adsorption on the $c(2 \times 2)$O/Co(100) heterostructure with estimated coverage reported in MLs.

The bottom spectrum of Fig. 1(a) is typical of a thick Co layer. The Cu substrate emission is fully suppressed, and the spectrum is dominated by Co 3d emission extending to about

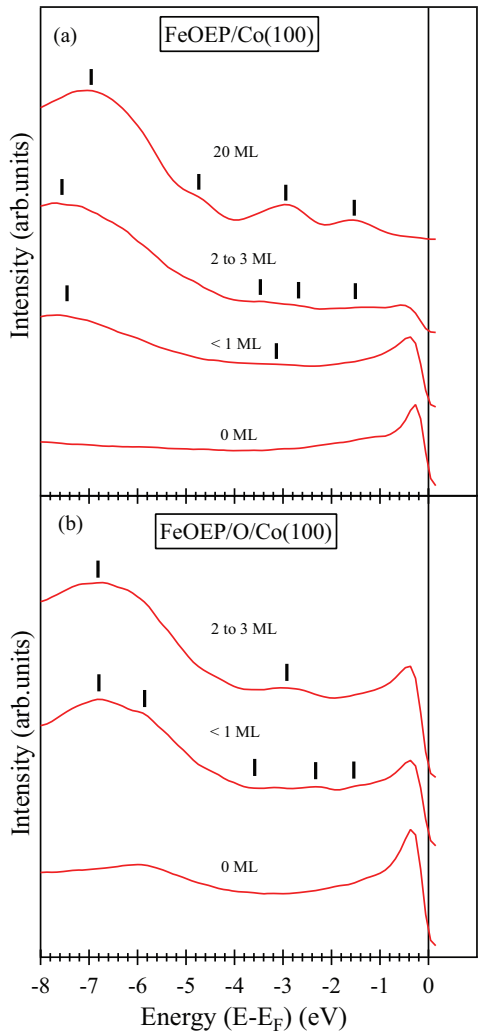

FIG. 1. (Color online) Top panel (a) spin-integrated energy dispersion curves of 10–15-ML Co/Cu(100) as a function of FeOEP coverage. Bottom panel (b) spin-integrated energy dispersion curves of O/Co/Cu(100) as a function of FeOEP coverage.

3 eV below the Fermi level. Upon oxygen exposure [Fig. 1(b), bottom spectrum], the Co $3d$ emission close to E_F is only weakly modified, whereas, the O $2p$ σ states appear at higher binding energies (about 6 eV).

For FeOEP exposures in the submonolayer region, the spectra for the two different substrates are quite dissimilar. On both substrates, new spectral densities appear around 3- and 7.5-eV binding energies (see the vertical bars), similar to reports of FePc adsorptions[27] yet distinct from the oxygen $2p$ photoemission intensity at 6 eV. Furthermore, in this submonolayer coverage, although the emission at 3 eV is very weak, a broad feature centered at 3.1 eV is formed in the case of the FeOEP adsorption on the Co(100), whereas, it clearly separates into two distinct features at 2.4 and 3.3 eV on the oxygen-treated surface. Moreover, the FeOEP/Co(100) spectral feature at 7.8-eV binding energy is at a distinctly higher binding energy than in the case of the FeOEP adsorption on the $c(2 \times 2)$O at 6.9 eV. At >1 ML coverage, the σ-based feature around 7.5 eV for both substrates shifts toward a lower binding energy. The orbital overlap between

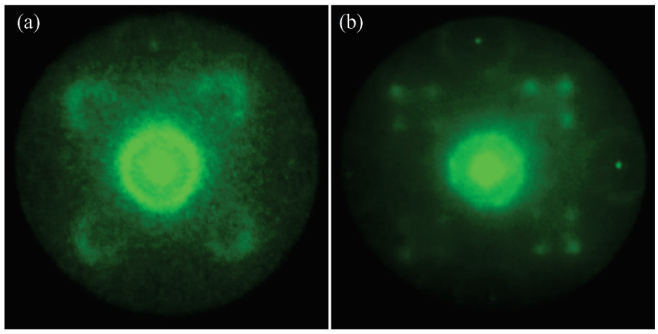

FIG. 2. (Color online) μ-LEED patterns recorded at 16 eV from ~1-ML FeOEP deposited on (a) Co/Cu(100) and (b) O/Co/Cu(100).

the nitrogen and the carbon of the FeOEP pyrrole rings with the substrate oxygen photoemission intensity suggests an exchange pathway, beyond the e_g^* bonding, between the molecules and the substrate. These different features are a first clue in understanding the exchange reversal mechanism between the FeOEPs on the two substrates.

Correspondingly, important differences also are observed in the μ-LEED. Figure 2 shows the μ-LEED patterns obtained from approximately 1 ML of FeOEP deposited on a clean Co/Cu(100) surface [Fig. 2(a)] and on the $c(2 \times 2)$ O/Co(100) [Fig. 2(b)]. On the clean metal, weak halos around the (00) spot as well as around the (1×1)-Co spots suggest the presence of a high degree of disorder. The film appears to be strongly textured with the formation of small domains, perhaps, of a few tens of nanometers in size, exhibiting short-range ordering of molecules but lacking long-range order.

The situation is very different in the case of the adsorption of submonolayer coverages of FeOEP molecules on the oxygen-covered surface [Fig. 2(b)]. In this case, the μ-LEED pattern is considerably sharper, indicating a much higher degree of ordering. This diffraction pattern resembles the $c(5\sqrt{2} \times \sqrt{2})R45^\circ$ superstructure. Now, the domains must be of several hundred nanometers with the intermolecular spacing (i.e., Fe-Fe distance) of 1.77 ± 0.1 nm. This behavior, which is due to an enhanced self-assembly, has also been observed in STM measurements of MnTPPCl molecules on a O/Co/Cu(100) surface.[28]

For coverages above a monolayer, new emission features start to appear in the photoemission spectra which eventually develop into distinct peaks at 1.5-, 3-, 4.5-, and 7.2-eV binding energies, respectively, at the 20-ML coverage. Interestingly, the double-peak feature in the submonolayer spectra of the oxygen-covered substrate merge into a single broad feature for coverages larger than 1 ML. On account of the surface sensitivity of our measurement, this is a first indication that the topmost Fe-porphyrin molecules are no longer interacting with the Co through O $2p$ states.

B. Spin-resolved valence-band photoemission spectra

Greater insight into the interfacial electronic structure is obtained from the spin-resolved photoemission spectra displayed in Figs. 3 and 4 with a direct relationship to the spin-integrated spectra shown in Fig. 1. The filled up-triangles indicate emission from majority-spin electrons, and

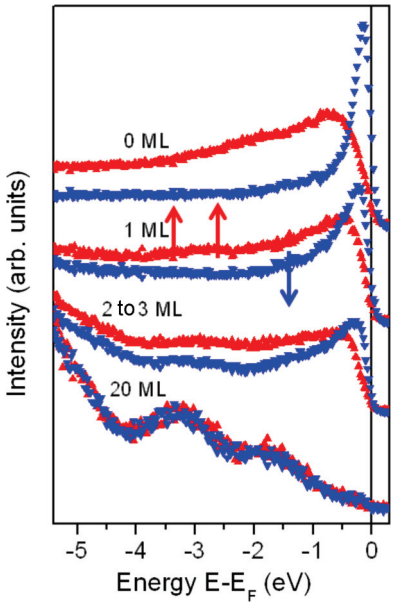

FIG. 3. (Color online) Spin-resolved spectra of Co/Cu(100) as a function of FeOEP coverage. The filled up-triangles correspond to the emission from the majority-spin direction, and the filled down-triangles correspond to the minority-spin direction of the cobalt thin film.

the filled down-triangles indicate emission from minority-spin electrons. As mentioned above, the SPPES studies were conducted with a large angular acceptance in order to minimize the incident photon flux and, therefore, the UV-beam damage of the molecules. Under these angle-integrated conditions, the photoemission intensity can be interpreted as a quantity proportional to the spin-resolved density of states (DOS).

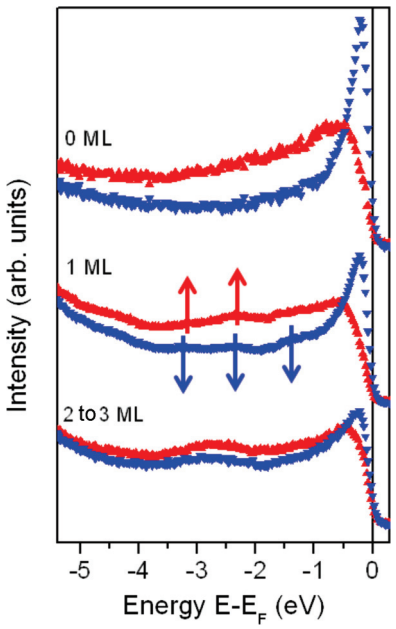

FIG. 4. (Color online) Spin-resolved spectra of O/Co/Cu(100) as a function of FeOEP coverage. The filled up-triangles correspond to the emission from the majority-spin direction, and the filled down-triangles correspond to the minority-spin direction of the Co(100) thin film.

The top spin-resolved spectra are for the Co substrate, clean (Fig. 3) or oxygen covered (Fig. 4). In both cases, the spectra are highly spin polarized and are indicative of a well-magnetized Co layer exhibiting a single ferromagnetic domain. The oxygenated surface has an overall lower spin polarization as one would expect.

Upon adsorption of a submonolayer of FeOEP on the clean metal (Fig. 3), a new feature emerging at around 3 eV is nearly all confined in the spin-up curve. This feature is very weak and broad, extending over more than 1 eV. Although not clearly resolved in the spectra, this feature is possibly composed of two states (marked with up-arrows), the broadening being a combination of strong hybridization and photoelectron scattering from disorder. A minority counterpart for these states can be seen in a small feature at approximately 1 eV in the minority spectrum (down-arrows). For comparison, we refer to the calculated Fe partial DOS (PDOS) of the FeP/Co(001) (Fig. 5). All three Fe spectral lines observed in the SPPES are seen in the calculated PDOS. The only main difference seems to be an overall shift of about 0.2 eV between the experimentally derived and the calculated results; overall, the agreement is very good.

Increasing the FeOEP coverage, the feature at ∼3 eV becomes even broader and, most importantly, loses its spin polarization. The remaining spin polarization is largely due to the underlying Co layer, which is now near the limit of depth sensitivity in a UV photoemission experiment at ∼3-ML coverage. The disappearance of the spin polarization in the FeOEP molecules is a clear indication that the magnetic ordering in the absorbed molecular layer is strictly induced by direct interaction of the molecules with the ferromagnetic substrate and is not able to self-support upon a second molecular layer. Indeed, the bottom spectrum is for a thick FeOEP layer where the photoelectron spin polarization is null.

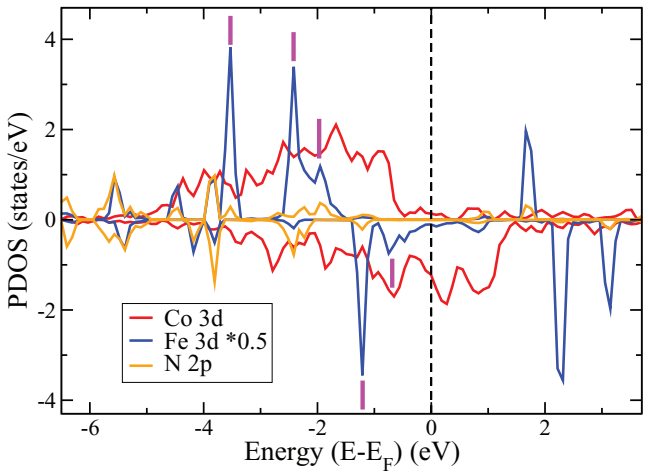

FIG. 5. (Color online) The DFT + U calculated spin-resolved partial DOS of FeP/Co(001), shown for ferromagnetic alignment of Co and Fe spins. Positive partial DOS corresponds to the majority Co(001) spin, and negative partial DOS corresponds to the minority spin. Van der Waals correction terms are not included in the calculation. The densities of Fe 3d (blue line), N 2p (tan line), and Co 3d (red line) orbitals are drawn. Vertical bars indicate regions of density discussed in the text.

The case of FeOEP deposition on the $c(2 \times 2)$O/Co(100) is shown in Fig. 4. As noted above, the atomic ordering is improved in this case, and all spectral features are sharper. Comparing the two spin-resolved spectra for submonolayer coverage in the two cases, one can clearly appreciate that there are major differences in the FeOEP molecules absorbed on the clean versus the oxygenated surface. The increased complexity is due to the oxygen-mediated interaction which results in a greater distribution of the Fe states over a larger energy range in an overall antiparallel magnetic coupling. Indeed, four distinct features are now distinguishable in the minority-spin spectrum, and three are distinguishable in the majority-spin spectrum [see Fig. 4 (up-arrows) and (down-arrows)]. This suggests that the spin-down states are more populated than the spin-up states, indicating an antiferromagnetic exchange coupling with the Co surface. Such antiferromagnetic exchange coupling was already unambiguously detected by element-selective x-ray magnetic circular dichroism (XMCD) measurements.[10] An antiferromagnetic coupling is also given by our DFT + U calculation, discussed below. The calculated Fe-DOS has, indeed, five main features in this energy region. The energy positions for FeP on oxygen-covered Co are, however, not as well reproduced, in particular, for the higher binding energy features.

In the case of an oxygen-reconstructed substrate, the magnetic exchange is again limited to the very first layer and has essentially disappeared already in the second layer, just as in the previous case. The μ-LEED and thickness-dependent SPPES results for both cases collectively show that the spin-polarized electronic structure of the overlayer is manifested more clearly when the molecular adsorptions are homogeneous in chemical and physical characters; furthermore, that the spin polarization of the molecular states exists only for molecules in the range of electron transfer with the substrate. We should, therefore, classify the relevant magnetic exchange in either system as driven by interfacial hybridization between the molecule and the substrate and nothing more (e.g., long-range dipole-dipole coupling).

C. Theoretical calculations

To clarify the origins of the observed magnetic and electronic interactions between the FeOEP and the Co substrate, we performed first-principles DFT + U calculations. From the DFT + U calculations for free-standing FeP molecules similar to the ones studied here, we found that a U value of 4 eV applied to the Fe atom and exchange interaction $J_{ex} =$ 1 eV provided good results.[9,20,21] The computational method is similar to that reported in Ref. 8, to which the reader is referred for details. In the present simulations, however, we have performed a complete structural relaxation of all molecular atomic distances, the $c(2 \times 2)$ reconstructed oxygen atoms as well as the top layer Co atoms, and the calculations were performed with and without VdW corrections.[24,25]

To start with, we consider FeP on the metallic Co substrate. Previous DFT + U calculations showed the molecule in the gas phase displays an intermediate spin $S = 1$ with a ground-state configuration corresponding to the $^3A_{2g}$ state.[9] Performing DFT + U calculations without VdW corrections for FeP adsorbed on Co, we obtain the same intermediate spin $S = 1$, which is coupled ferromagnetically to the spin of the Co surface atoms. However, if we precisely perform the same calculations with VdW corrections, we obtain a high spin $S \approx 2$ for FeP adsorbed on Co. Figure 5 shows the spin-resolved PDOS, computed with the DFT + U approach without VdW corrections for FM alignment between Co and Fe moments at an optimal Co and Fe distance of 3.52 Å. Performing the same optimization with VdW corrections leads to a much stronger Fe-Co bonding at a much shorter distance of 2.41 Å. The spin-resolved PDOS for this situation is shown in Fig. 10 and is discussed in the Appendix. As we observed that the inclusion of the VdW correction worsens the agreement with experiment, we discuss first results of the DFT + U calculation without such a correction.

Figure 5 illustrates that there exists hybridization between Fe 3d and N 2p states; specifically, between $3d_{x^2-y^2}$ and $3d_\pi$ (d_π is the result of hybridizing d_{xz} and d_{yz}) states with N $2p_z$ states as projections on the orbital character show.[21] Moreover, the calculation of Wende *et al.*[8] has shown that these N 2p hybridized peaks follow the Fe 3d spin polarization when Fe coupling changes from FM to AFM. Although the Fe-Co distance of 3.52 Å is considerably large for direct overlap between Co 3d and Fe 3d states, we find a clear interaction of the Fe d_{z^2} state with the Co Δ_5 ($\downarrow$) state at 0.5 eV below E_F, which leads to strong broadening of the d_{z^2} orbital. This broadening of the d_{z^2} orbital was not observed by Wende *et al.*, likely because they did not perform a complete geometrical relaxation of the atomic distances. A small N-Co hybridization can be observed at 2.4-eV binding energy. This shows that there is a strong chemical binding of molecules to the Co substrate through N p_z orbitals as proposed in Ref. 8. The computed atomic spin moments are 2.08 μ_B on Fe and $-0.026\,\mu_B$ on each of the nitrogen atoms, giving a total spin $S \approx 1$ on the molecule.

The peak structures in the spin-resolved PES at the submonolayer coverage of Fig. 3 can be compared directly to the DFT + U partial DOS in Fig. 5. The measured data show the appearance of two broad peaks at about 2.6 and 3.7 eV in the spin-majority spectrum. These peaks compare well with the computed spin-up Fe 3d peaks at 2.4- and 3.7-eV binding energies (denoted by vertical bars). In the minority-spin photoemission spectrum, a small peak develops at 1.5-eV binding energy. This peak corresponds well with an Fe 3d peak due to the d_{xy} orbital presented at 1.3-eV binding energy (Fig. 4). DFT + U theory predicts a small and broadened spin-down DOS due to the hybridized d_{z^2} orbital at about 0.7-eV binding energy. This might be reflected in the broadening of the low-energy minority-spin emission peak appearing in the measured data.

The overall agreement between DFT + U calculated and measured SPPES peak positions is, nonetheless, reasonably good. Counterintuitively, the agreement between calculated and measured spin-polarized densities is lost when the VdW correction is included; this is discussed in more detail in the Appendix. Furthermore, as the peak positions predicted by the common DFT approach in the generalized gradient approximation (i.e., $U = 0$) differ substantially[9,27] from those obtained with the DFT + U method, it can be concluded that the latter approach predicts an electronic structure of adsorbed metalloporphyrins that corroborates with experiments.

Next, we consider adsorption of iron porphyrin on the oxygen $c(2 \times 2)$ reconstructed Co(001) surface. In the present

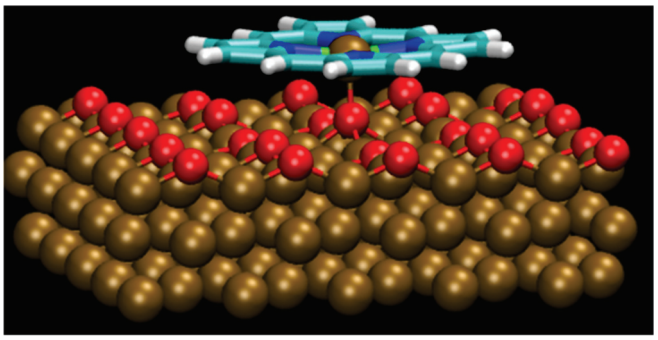

FIG. 6. (Color online) The structurally optimized geometry of iron porphyrin on a $c(2 \times 2)$ oxygen-reconstructed Co(001) surface. Co and Fe atoms are denoted by the larger (brown) balls, oxygen atoms are depicted by the smaller (red) balls. Note the upward displacement of the oxygen atom under the Fe center of the porphyrin molecule, caused by apical ligand formation to the Fe center.

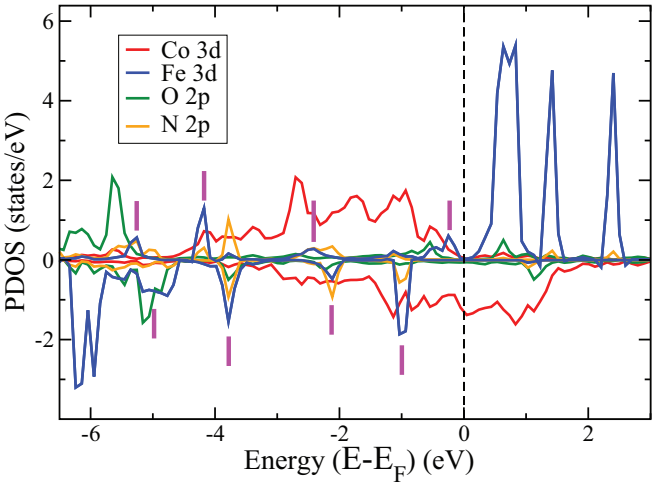

FIG. 7. (Color online) The DFT + U calculated spin-resolved partial DOS of FeP on $c(2 \times 2)$ oxygen-reconstructed Co(001), shown for an antiferromagnetic alignment of Co and Fe spins. Positive partial DOS corresponds to the Co(001) majority spin, negative partial DOS corresponds to the minority spin. The densities of Fe 3d (blue line), N 2p (tan line), O 2p (green line), and Co 3d (red line) orbitals are drawn. Vertical bars indicate regions of density discussed in the text. Van der Waals correction terms are not included in the calculation.

DFT + U calculations, a full geometrical optimization of the FeP on the oxygen-reconstructed $c(2 \times 2)$ surface was performed. In this case, we do not find a notable difference between calculations with or without VdW corrections. In the previous study,[10] only bonding of Co to Fe through a single oxygen atom on top of the Co atom was considered, whereas, here, the full $c(2 \times 2)$ oxygen reconstruction was treated. We find that the structural optimization has a clear effect on the oxygen positions. As illustrated in Fig. 6, several oxygen atoms beneath the porphyrin molecule move out of their $c(2 \times 2)$ adsorption positions. In particular, the oxygen atom underneath the central Fe ion of the metalloporphyrin moves up, which signals an increased bonding of this oxygen to the iron in the free out-of-plane ligand position. The Fe-O distance is 2.08 Å. The computed magnetic moment on the Fe in FeP is in this configuration $-3.99\ \mu_B$ with $-0.06\ \mu_B$ on each of the nitrogens and $0.05\ \mu_B$ on the underlying oxygen atom. Hence, the molecule's spin is approximately 2, implying that the spin of FeP (without an apical Cl ligand) has switched from intermediate $S = 1$ in the gas phase to high spin $S \approx 2$ upon adsorption on O/Co(001). The adsorbed oxygen atoms on the clean surface of Co have an induced moment of $\sim 0.18\ \mu_B$ per O atom. Moreover, the spin on the FeP is coupled antiparallel to the spin on the Co atoms. An antiparallel coupling has been reported previously.[10] As pointed out,[10] this coupling can be attributed to an indirect exchange coupling between Fe and Co spins, mediated by the bridging oxygen atom.

The computed partial DOS is shown in Fig. 7 (shown are the spin-resolved PDOS computed without VdW correction). The positions of the spin-polarized DOS peaks can be compared to the spin-polarized photoemission data in Fig. 4. In the measured spin-minority spectrum, a peak develops with a binding energy of about 1.4 eV for submonolayer coverage. This peak compares well with the Fe-3d peak present in the computed partial DOS at 1-eV binding energy. Other new structures appear in both the measured spin-minority and the spin-majority spectra at about 2.4-eV binding energy. These peaks correspond to Fe- and N-related DOS features that are present in both spin channels at about 2–2.5-eV binding energies. The next features in the measured photoemission spectra appear at 3.5-eV binding energy, again, in both spin channels. These structures find their theoretical counterparts in Fe and N partial DOS peaks appearing between 3.5 and 4.2 eV in both spin channels. Also, a stronger increase in the spin-polarized photoemission signal can be seen in the data at about 5 eV, which is at the lower end of the measured spectra. A similar upturn of the signals, notably, is not detected for FeOEP on Co(100) (see Fig. 3). This upturn could be explained by the presence of deep-lying Fe 3d states at 5- to 6-eV binding energies for the oxygen-reconstructed surface, which are not present for FeP on the Co(001) surface. DFT + U theory also predicts a spin-majority Fe 3d peak just below the Fermi energy, but identification of this feature is difficult due to the reducing effect of the Fermi edge on the spectra at binding energies less than 0.5 eV. The agreement between the SPPES peak positions and the calculated peaks is overall not as good for FeOEP on oxygen-reconstructed Co as it is for FeOEP on Co. A reason for this might be that, in the measurement, some FeOEP molecules could exist at adsorption sites other than the iron-atop-oxygen location.

IV. CONCLUSIONS

By means of spin-resolved photoemission spectroscopy, we have directly probed the spin-polarized occupied electronic structure of FeOEP molecules on a metallic and on an oxygen-reconstructed Co(100) surface. For all the molecular coverages studied, we found that the induced spin polarization is only in the submonolayer region. For FeOEP, a FM exchange coupling to Co(100) was identified. Through comparison with results from DFT + U calculations, an AFM exchange coupling to O/Co(100) was identified, consistent with earlier measurements.[10] The spin-polarized photoemission of FeOEP/Co/Cu suggests FM coupling due to the presence of

minority band peaks at 1.5 and 2.9 eV and majority band peaks at 2.6 and 3.7 eV below E_F. The positions of these peaks are relatively well explained by DFT + U calculations, albeit that the peaks in the PDOS calculation are shifted by up to 0.4 eV (mostly by 0.2 eV) in comparison to the measured data. This good agreement substantiates the need for including the Coulomb U to attain the proper electronic structure description of Fe porphyrins. Furthermore, we find that inclusion of VdW corrections surprisingly worsens the correspondence with measured SPPES spectra.

The spin-polarized photoemission of FeOEP/O/Co/Cu suggests AFM coupling due to the presence of minority band peaks at 2.4 and 3.3 eV and majority band peaks at 2.3 and 3.2 eV below E_F. A prominent minority band peak also appears at 1.4 eV below E_F. The energy positions of these measured peaks compare relatively well to peak structures in the DFT + U computed PDOS for FeP on O/Co(001). For FeP/O/Co(001), there also exist shifts in the computed energies as compared to the measured energy positions of up to 0.5 eV. The overall agreement between the spin-polarized photoemission experiment and the DFT + U theory can, nonetheless, be regarded as fairly good. Our investigations exemplify that the exchange mechanism is considerably different in the cases of AFM coupling and FM coupling.

ACKNOWLEDGMENTS

We would like to thank G. Nintzel and M. Caruso at NSLS for valuable technical assistance. Experimental work was performed at Brookhaven National Laboratory, which is supported by the US Department of Energy (DOE) under Contract No. DE-AC02-98CH10886. Financial support from the Swedish Research Council, the Swedish-Indian Research Links Program, and the National Science Foundation (Grant No. DMR-1005882) is thankfully acknowledged. Support from the Swedish National Infrastructure for Computing (SNIC) is also acknowledged.

APPENDIX

In general, Van der Waals corrections[14,29,30] are expected to improve the description of metal-organic molecules adsorbed on surfaces. For CoPc on an Fe(110) surface, a considerable shortening of the molecule-surface distance due to VdW corrections was reported.[13] Our results of DFT + U + VdW calculations are summarized in the following.

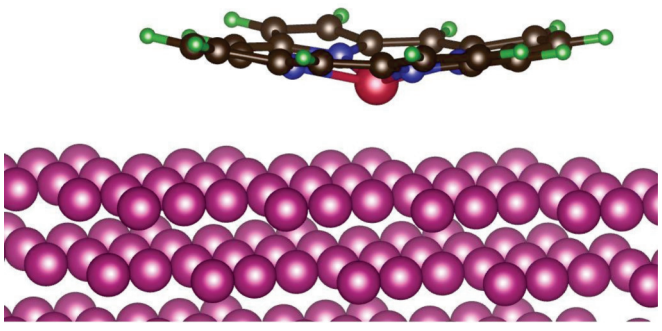

FIG. 8. (Color online) Fully relaxed geometry of the Fe porphyrin molecule on Co(001), computed with the DFT + U method and inclusion of Van der Waals corrections. Note the bend conformation with the Fe atom displaced out of the macrocyclic plane. Green spheres depict hydrogens, blue spheres depict nitrogens, dark gray spheres show carbons, the red sphere depicts iron, and purple spheres depict cobalt atoms.

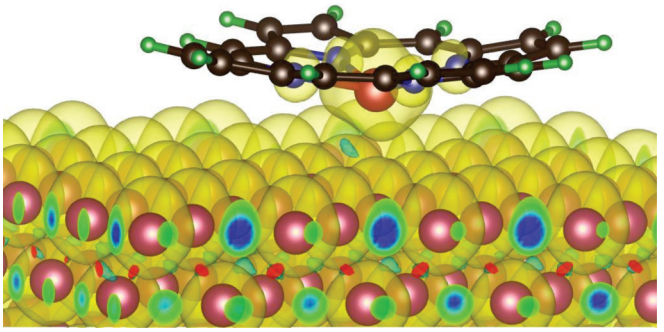

FIG. 9. (Color online) Computed magnetization density of the same system. The yellow isosurfaces represent the positive magnetization direction.

Including VdW corrections, we find, too, that the FeP molecule is drawn closer to the top Co layer (Fe-Co distance of 2.41 Å) but, additionally, that the molecule's geometry becomes bent with the Fe ion being displaced toward the surface out of the macrocyclic plane; the Fe-N bond lengths are 2.12 Å. The optimized molecular geometry is shown in Fig. 8. The calculations predict the iron porphyrin and Co surface to be strongly ferromagnetically coupled. In addition to the stronger coupling with the Co surface, the FeP molecule is found to be in the high-spin state $S \approx 2$ (with projected atomic moments of 3.7 μ_B on Fe and 0.05 μ_B on each of the nitrogen atoms). The *ab initio* computed high-spin state would imply that iron porphyrin would switch from intermediate $S = 1$ spin in the gas phase to high spin on the Co surface. The computed magnetization density is shown in Fig. 9. The magnetization densities on the Fe and nitrogen atoms are parallel in contrast to what was calculated previously for free

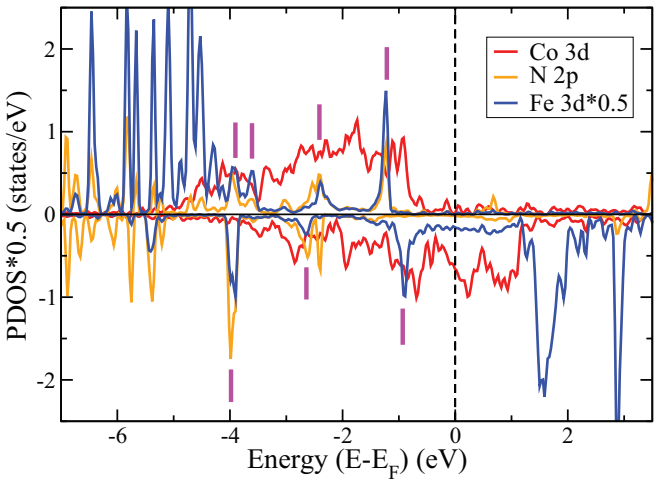

FIG. 10. (Color online) The spin-resolved partial DOS of FeP/Co(001), computed with the DFT + U formalism and inclusion of Van der Waals correction terms. The spin-resolved densities of Fe 3d (blue line), N 2p (tan line), and Co 3d (red line) orbitals are shown. Vertical bars indicate the peak positions of the Fe 3d DOS (below 4 eV).

FeP or for FeP adsorbed on Co with DFT + U without VdW terms.[8] A possible way to experimentally verify which spin polarization direction is actually realized on the nitrogens would be to employ element-selective XMCD measurements.

The calculated spin- and atom-resolved DOS is shown in Fig. 10. The main positions of Fe 3d DOS peaks are highlighted by the vertical bars. The calculated Fe 3d positions differ substantially from those computed without VdW terms (Fig. 5): a strong Fe-3d peak is present in the spin-majority channel at −1.2 eV, and another significant peak is present in the spin-minority channel at −4 eV. Notably, these structures are not present in the measured SPPES spectra (Fig. 3) and, altogether, there is practically no correspondence between the computed and the measured peak positions. The VdW corrections evidently lead to a much stronger binding of the FeP molecule to the surface, but, as the thus-obtained spin-polarized PDOS do not correspond with the SPPES data, the effect appears to be too strong. A tendency of VdW corrections to exaggerate the bonding has been reported previously.[25] Our results obviously do not alleviate the need for VdW corrections but rather pinpoint that further improvements of VdW DFT functionals are to be sought.

*Author to whom all correspondence should be addressed: carusoan@umkc.edu

[1] J. Zaanen, G. A. Sawatzky, and J. W. Allen, Phys. Rev. Lett. **55**, 418 (1985).
[2] A. Scheybal, T. Ramsvik, R. Bertschinger, M. Putero, F. Nolting, and T. A. Jung, Chem. Phys. Lett. **411**, 214 (2005).
[3] N. Atodiresei, J. Brede, P. Lazić, V. Caciuc, G. Hoffmann, R. Wiesendanger, and S. Blügel, Phys. Rev. Lett. **105**, 066601 (2010).
[4] U. G. E. Perera, H. J. Kulik, V. Iancu, L. G. G. V. Dias da Silva, S. E. Ulloa, N. Marzari, and S.-W. Hla, Phys. Rev. Lett. **105**, 106601 (2010).
[5] V. A. Dediu, L. E. Hueso, I. Bergenti, and C. Taliani, Nat. Mater. **8**, 707 (2009).
[6] S. Lach *et al.*, Adv. Funct. Mater. **22**, 989 (2012).
[7] P. Gambardella *et al.*, Nat. Mater. **8**, 189 (2009).
[8] H. Wende *et al.*, Nat. Mater. **6**, 516 (2007).
[9] P. M. Panchmatia, B. Sanyal, and P. M. Oppeneer, Chem. Phys. **343**, 47 (2008).
[10] M. Bernien *et al.*, Phys. Rev. Lett. **102**, 047202 (2009).
[11] M. Bernien *et al.*, Phys. Rev. B **76**, 214406 (2007).
[12] F. de Groot and A. Kotani, *Core Level Spectroscopy of Solids* (CRC, Boca Raton, FL, 2008).
[13] J. Brede, N. Atodiresei, S. Kuck, P. Lazić, V. Caciuc, Y. Morikawa, G. Hoffmann, S. Blügel, and R. Wiesendanger, Phys. Rev. Lett. **105**, 047204 (2010).
[14] S. Stepanow, P. S. Miedema, A. Mugarza, G. Ceballos, P. Moras, J. C. Cezar, C. Carbone, F. M. F. de Groot, and P. Gambardella, Phys. Rev. B **83**, 220401(R) (2011).
[15] W. Clemens, E. Vescovo, T. Kachel, C. Carbone, and W. Eberhardt, Phys. Rev. B **46**, 4198 (1992).
[16] K. Baberschke, J. Phys. Conf. Ser. **190**, 012012 (2009).
[17] S. Kuck, M. Prostak, M. Funk, M. Bröring, G. Hoffmann, and R. Wiesendanger, J. Vac. Sci. Technol. A **28**, 795 (2010).
[18] P. D. Johnson, N. B. Brookes, S. Hulbert, R. Klaffky, A. Clarke, B. Sinkovic, N. V. Smith, R. Celotta, M. H. Kelly, D. T. Pierce, M. R. Scheinfein, B. J. Waclawski, and M. R. Howells, Rev. Sci. Instrum. **63**, 1902 (1992).
[19] E. Vescovo *et al.*, Activity Report 1996, Nat. Synch. Light Source, A-25 (1997).
[20] P. M. Panchmatia, M. E. Ali, B. Sanyal, and P. M. Oppeneer, J. Phys. Chem. A **114**, 13381 (2010).
[21] M. E. Ali, B. Sanyal, and P. M. Oppeneer, J. Phys. Chem. B **116**, 5849 (2012).
[22] G. Kresse and J. Furthmüller, Phys. Rev. B **54**, 11169 (1996).
[23] P. M. Oppeneer *et al.*, Prog. Surf. Sci. **84**, 18 (2009).
[24] S. Grimme, J. Comput. Chem. **27**, 1787 (2006).
[25] T. Bucko, J. Hafner, S. Lebègue, and J. G. Ángyán, J. Phys. Chem. A **114**, 11814 (2010).
[26] J. P. Perdew, K. Burke, and M. Ernzerhof, Phys. Rev. Lett. **77**, 3865 (1996).
[27] B. Brena *et al.*, J. Chem. Phys. **134**, 074312 (2011).
[28] D. Chylarecka *et al.*, J. Phys. Chem. Lett. **1**, 1408 (2010).
[29] A. Tkatchenko and M. Scheffler, Phys. Rev. Lett. **102**, 073005 (2009).
[30] J. D. Baran and J. A. Larsson, J. Phys. Chem. C **116**, 9487 (2012).